

SUPERCONDUCTING RF ACTIVITIES FOR THE RARE ISOTOPE ACCELERATOR AT MICHIGAN STATE UNIVERSITY*

T. L. Grimm, V. Andreev, J. Bierwagen, S. Bricker, C. Compton, D. Gorelov, W. Hartung, M. Johnson, F. Marti, S. Schriber, X. Wu, R. C. York, and Q. Zhao
 National Superconducting Cyclotron Laboratory, Michigan State University, East Lansing MI
 P. Kneisel and G. Ciovati
 Thomas Jefferson National Accelerator Facility, Newport News VA
 A. Facco
 INFN – Laboratori Nazionali di Legnaro, Padova Italy

INTRODUCTION

Since 2001, Michigan State University (MSU), in collaboration with Jefferson Lab (JLAB) and INFN-Legnaro, has been carrying out R&D on the driver linac and post-accelerator linac for the Rare Isotope Accelerator (RIA). This includes construction of prototypes of all cavity types and cryomodules for testing under realistic operating conditions. The cryomodules include tuners, power couplers, microphonics control elements, and focusing magnets. Prototypes of all cavity types have been successfully demonstrated, and cryomodules are under construction. By the end of 2004, all linac R&D should be complete so that designs, production plans and costing of RIA can be finalized.

RIA LINAC DESIGNS

The RIA facility employs two superconducting linacs to accelerate heavy ions [1-3]. The driver linac is used to accelerate up to 400 kW CW heavy ion beams of uranium to 400 MeV per nucleon or lighter ions such as protons to over 1 GeV. Because of the varying velocity of the beam along the linac, a number of different types of superconducting RF structures are needed. The post-accelerator is used to accelerate low intensity radioactive (or rare) isotopes to about 10 MeV/u; it will use the same low velocity structures developed for the driver linac.

The simplicity of the superconducting linacs presented here allows demonstration of all cavity and cryomodule types within the limited RIA R&D budget and short time scale before RIA construction, thereby significantly reducing the uncertainty and risk to the project schedule

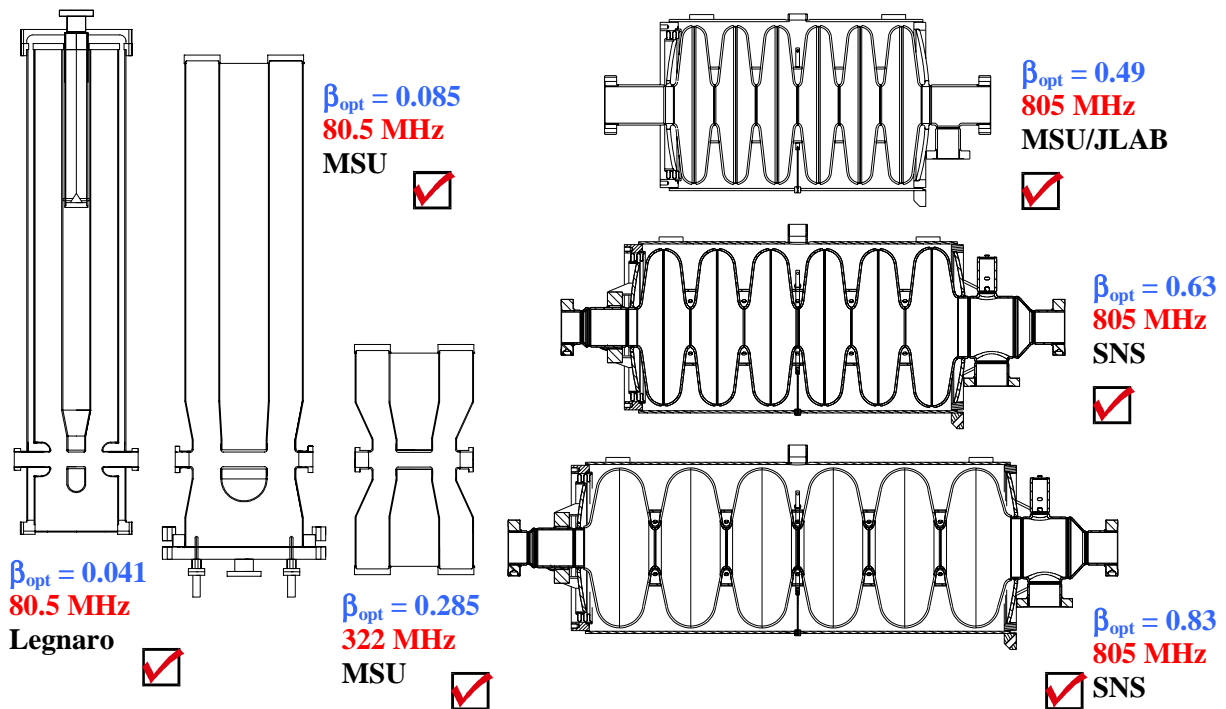


Figure 1: Superconducting RF cavities for RIA.

* Work supported by the U.S. Department of Energy under grant numbers DE-FG02-03ER41247 and DE-FG02-03ER41248.

and cost. The cavity types are shown in Figure 1, and their design parameters are given in Table 1. Figures 2 and 3 show the transit time and energy gain as a function of β (the beam velocity v divided by the speed of light c) for uranium and protons, respectively.

Beam dynamics calculations have shown that the RFQ acceptance and output emittance is well matched to the driver linac [4]. Longitudinal and transverse beam dynamics simulations of the entire linac show adequate longitudinal and transverse acceptance including alignment errors, RF jitter, and stripper foil energy straggling [5-7].

SCDTL

The low-energy section of the driver linac uses superconducting cavities to accelerate beam from $\beta \sim 0.025$ (0.3 MeV/u) to $\beta \sim 0.4$ (85 MeV/u), which constitutes about one-quarter of RIA's total accelerating voltage. MSU has considered various alternative designs and optimization strategies, and has determined that a 10th harmonic linac based on 80.5 MHz is an attractive solution. To minimize R&D and technical risk, the superconducting drift tube linac (SCDTL) has a minimum number of cavity types and uses passive microphonics control. Three cavity types can cover the velocity range if they are two-gap structures.

The cavity for the lowest velocity particles has the smallest accelerating gaps, and thus has the most severe issues with control of microphonics. Therefore, an 80.5

Table 1: RIA cavity design parameters: β_{opt} is the optimum β , f is the resonant frequency, V_a is the voltage per cavity (at $\beta = \beta_{\text{opt}}$, including transit time effects), T is the operating temperature, Q_0 is the quality factor, P_0 is the power dissipation per cavity, R/Q is the geometric shunt impedance per cavity, G is the geometry factor, R_s is the RF surface resistance, and E_p and B_p are the peak surface electric and magnetic fields, respectively.

| Type | $\lambda/4$ | $\lambda/4$ | $\lambda/2$ | 6-cell | 6-cell | 6-cell |
|----------------------|-----------------|-------------|-----------------|-----------------|--------------------|----------------------|
| β_{opt} | 0.041 | 0.085 | 0.285 | 0.49 | 0.63 | 0.83 |
| f (MHz) | 80.5 | | 322 | 805 | | |
| V_a (MV) | 0.46 | 1.18 | 1.58 | 5.12 | 8.17 | 13.46 |
| T (K) | 4.5 | | 2 | 2 | | |
| Q_0 | 5×10^8 | | 5×10^9 | 8×10^9 | 1×10^{10} | 1.2×10^{10} |
| P_0 (W) | 1.0 | 6.7 | 2.5 | 19.0 | 23.9 | 31.3 |
| R/Q (Ω) | 424 | 416 | 199 | 173 | 279 | 483 |
| G (Ω) | 15.7 | 19.0 | 61.0 | 155 | 180 | 260 |
| R_s (n Ω) | 31.4 | 38.0 | 12.2 | 19.4 | 18.0 | 21.7 |
| E_p (MV/m) | 16.5 | 20 | 25 | 32.5 | 32.5 | 32.5 |
| B_p (mT) | 28.2 | 46.5 | 68.6 | 64.2 | 68.6 | 70.2 |
| Aperture (mm) | 30 | | | 77 | 86 | 98 |
| Magnets | NbTi solenoids | | | Cu quads | | |
| # cavities | 18 | 104 | 208 | 68 | 64 | 32 |
| # cryo-modules | 2 | 13 | 26 | 17 | 16 | 8 |

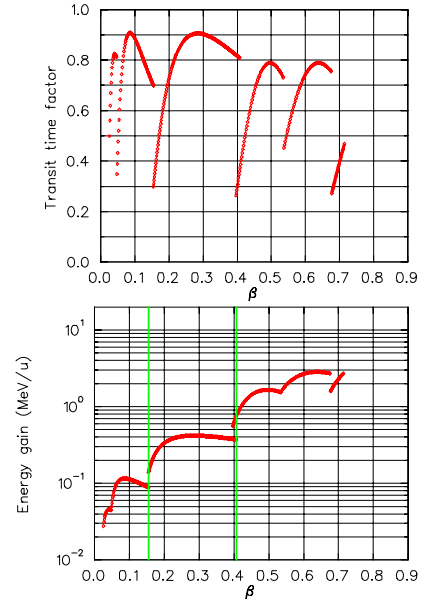


Figure 2: Transit time factor and energy gain for uranium.

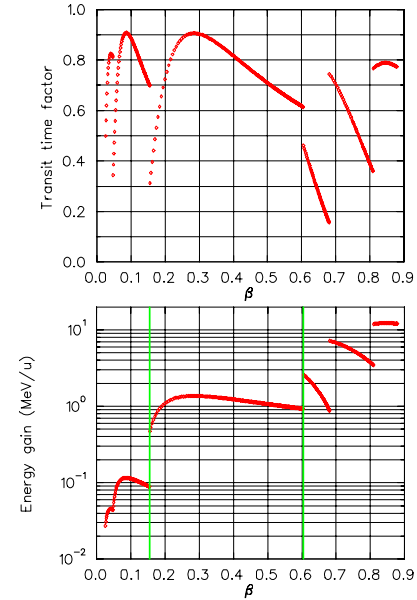


Figure 3: Transit time factor and energy gain for protons.

MHz $\beta_{\text{opt}} = 0.041$ quarter wave resonator (QWR) very similar to that already developed for INFN-Legnaro's heavy ion linac is used [8]. Microphonics are controlled with a passive mechanical damper whose effectiveness has been proven above 80 MHz, instead of active control with VCX or piezoelectric fast tuners. The second cavity type is an 80.5 MHz $\beta_{\text{opt}} = 0.085$ QWR with reduced microphonics due to its larger diameter. The final cavity type is a 322 MHz $\beta_{\text{opt}} = 0.285$ half-wave resonator (HWR).

The SCDTL lattice maintains microphonic control with passive mechanical dampers and RF drive. This avoids the need for VCX tuners that have several disadvantages for operation in a large linac [9]. The SCDTL lattice uses smaller and simpler cavities (relative to ANL's 57.5 MHz

version) that will be more easily fabricated at lower cost. Although the higher frequency lattice will require more units, it is anticipated that the overall system costs will be comparable for either SCDTL.

Elliptical Cavity Linac

The high-energy section of the driver linac uses elliptical cavities to accelerate beam from $\beta \sim 0.4$ (85 MeV/u) to $\beta \geq 0.72$ (400 MeV/u), which constitutes about three-quarters of RIA's total accelerating voltage [1]. A significant synergistic advantage was realized with the decision to utilize the 805 MHz elliptical, axisymmetric, 6-cell cavities with geometric β values (β_g) of 0.61 and 0.81 developed for the Spallation Neutron Source (SNS), thereby saving the non-recurring development and engineering costs, and reducing technical risk [2, 10]. For additional savings, it was decided to extend the elliptical multi-cell cavity design to lower velocity, $\beta = 0.4$. The development of an 805 MHz $\beta_g = 0.47$ six-cell cavity was undertaken as a collaboration between MSU, JLAB, and INFN-Milan.

The design gradient of 9.7 MV/m for the $\beta_g = 0.47$ cavity corresponds to $E_p = 32.5$ MV/m and $B_p = 64$ mT. These are less than the design values for the SNS cavities ($E_p = 35$ MV/m and $B_p = 76$ mT). One important advantage associated with the use of elliptical cavities is the large beam aperture (77 mm), which minimizes beam loss, relaxes alignment criteria, and eliminates the need for additional higher-order-mode couplers.

CAVITY PROTOTYPING

Three cavity types have been prototyped specifically for RIA. Figure 4 shows the completed cavities and the parts for one of the cavities prior to welding. Figure 5 shows the RF test results for the three cavities.

SCDTL Cavities

Since the $\beta_{opt} = 0.041$ QWR is very similar to an existing Legnaro design, only two SCDTL cavities (with common diameters for the inner and outer conductor) needed to be prototyped. A prototype of the 80.5 MHz $\beta_{opt} = 0.085$ QWR cavity was fabricated and tested in the Fall of 2003 [11]; it significantly exceeded the required quality factor and accelerating field (Figure 5, squares). A prototype 322 MHz $\beta_{opt} = 0.285$ HWR was fabricated and tested in 2002 [12]; it also exceeded the design goals by a significant margin (Figure 5, diamonds). These experimental results justify the design values of $E_p = 16.5$ to 25 MV/m for the SCDTL given in Table 1, especially with isolated vacuum. In addition, the design quality factors of 5×10^8 for the QWRs and 5×10^9 for the HWR at 2 K include reasonable safety factors. Note that the first QWR uses very conservative values for added reliability, since there are so few units.

Elliptical Cavities

With the $\beta_g = 0.61$ and $\beta_g = 0.81$ cavities already in production for SNS, the only elliptical cavity to be



Figure 4: Top: parts for 80.5 MHz QWR (left) and inside view of completed cavity (right). Bottom: 80.5 MHz QWR (left), 322 MHz HWR (middle) and 805 MHz 6-cell (right) on their RF test stands.

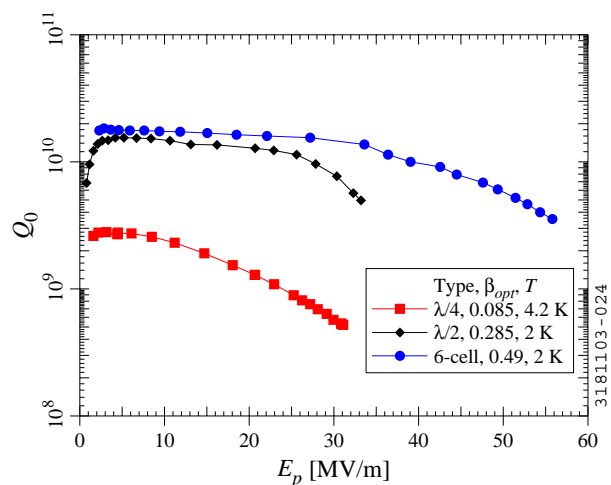


Figure 5: RF test results for the 80.5 MHz QWR (4.2 K), the 322 MHz HWR (2 K) and the 805 MHz 6-cell (2 K).

prototyped for RIA was the $\beta_g = 0.47$ six-cell cavity. Two single-cell units were made first, following the design of Barni *et al.* [13]. Their performance significantly exceeded the goals for RIA [14].

Next, a simplified six-cell prototype (no radial couplers, stiffeners, tuner, or helium vessel) was fabricated to test the electromagnetic performance, frequency, field flatness, and microphonic response [15]. The cavity was

mechanically tuned to $\sim 10\%$ field unflatness before processing and assembly in a Class 100 clean room. The cavity was tested in September 2002 (Figure 5, circles). As can be seen in Figure 5, the design value maintains a significant safety factor. The design accelerating gradient with a Q_0 of 8×10^9 would generate 19 W of heating per six-cell cavity.

The final R&D phase for cavity fabrication was the construction of two six-cell prototypes with stiffening rings, coupler ports, and He vessel dishes. Testing of these units in a vertical cryostat configuration was completed in May 2003 with results comparable to the simple six-cell [15].

CRYOMODULE DEVELOPMENT

A rectangular cryomodule design with cryogenic alignment rail that can accommodate all of the superconducting cavity and magnet types is proposed for RIA [16]. The SNS cryomodule could be used for the RIA elliptical cavity linac, but this would be inappropriate for the RIA SCDTL, and significant simplifications and cost savings are possible with the rectangular cryomodule due to RIA's continuous, relatively low power beam.

Elliptical Cavity Cryomodule

The cryomodule design is shown in Figure 6. Beam dynamics simulations show that four $\beta_g = 0.47$ cavities per module are acceptable. A prototype cryomodule for two cavities is under construction. The cavities, helium vessels, power couplers and tuners have been completed, as shown in Figure 7.

Given RIA beam loading and an estimated required microphonic-driven bandwidth, a Q_{ext} value of approximately 2×10^7 was chosen for the input coupling. MAFIA and ANALYST simulations of possible coupler configurations were confirmed with tests using the single-cell and multi-cell copper models. The final coupler design is only a slight modification of the SNS coupler. An analysis was done and a determination made that no HOM dampers will be required for the RIA driver linac [17]. Two power couplers have been fabricated and conditioned to 200 kW [18,19].

In the cryomodule tests, issues such as attainable gradient, cryogenic load and control of microphonics will

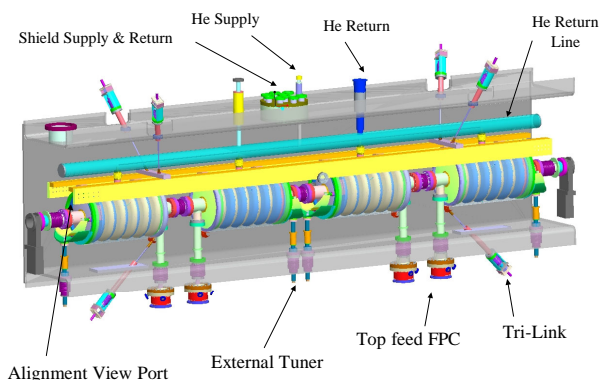


Figure 6: The $\beta_g = 0.47$ cryomodule design.

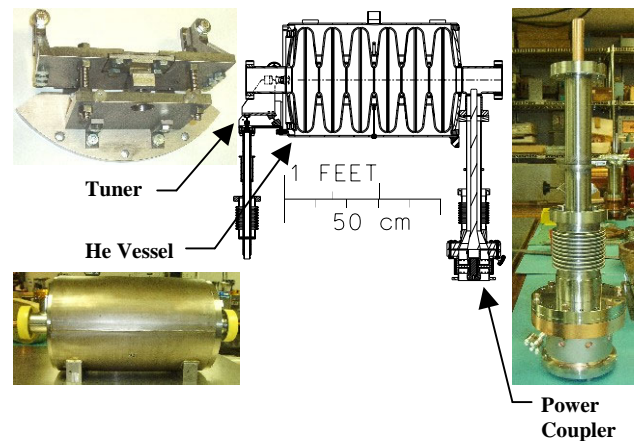


Figure 7: Six-cell $\beta_g = 0.47$ cavity with radial coupler ports, stiffening rings, He vessel, tuner and input power coupler.

be addressed, and the performance of the mechanical tuner, power coupler, and RF system will be checked. As RIA and the CEBAF upgrade have comparable beam loading and Q_{ext} , the techniques used for CEBAF should be applicable to RIA. Passive and active microphonics control schemes are also being explored.

The prototype cryomodule assembly should be complete in 2003. Figure 8 shows the two 6-cell cavities being test fit on the titanium alignment rails and the magnetic shield being test fit below the top plate of the vacuum vessel. Testing under realistic operating conditions will take place in 2004.

SCDTL Cryomodule

The cryomodules for the SCDTL have been designed, including tuners and superconducting solenoids. The design is very similar to the rectangular cryomodule for the elliptical cavities. Figure 9 shows the cryomodule for the 322 MHz $\beta_{opt} = 0.285$ HWR with 9 T superconducting solenoids. A prototype cryomodule containing all cavity and solenoid types is shown in Figure 10. Prototype cryomodule construction and testing are planned for 2004.

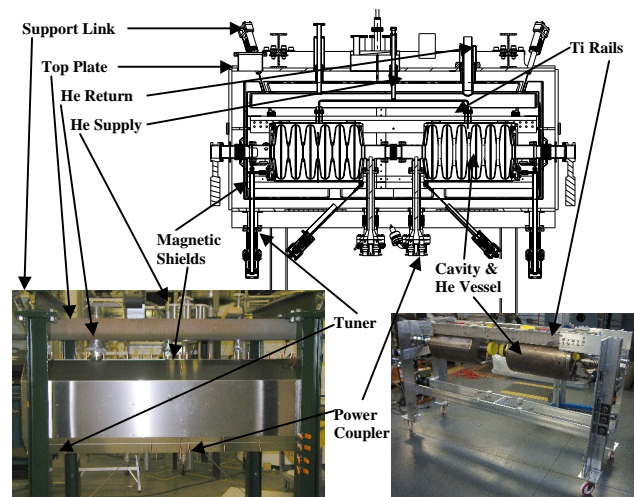


Figure 8: Prototype cryomodule for two $\beta_g = 0.47$ cavities.

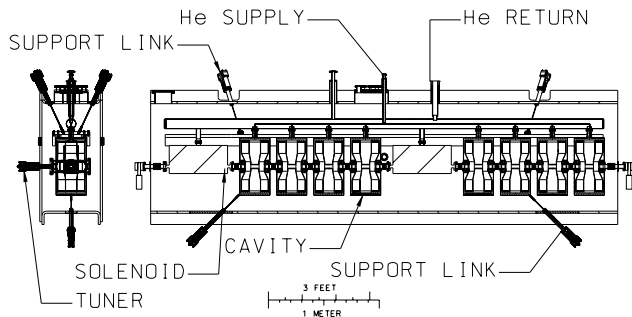


Figure 9: Horizontal cryomodule for the 322 MHz $\beta_{\text{opt}} = 0.285$ half-wave resonator.

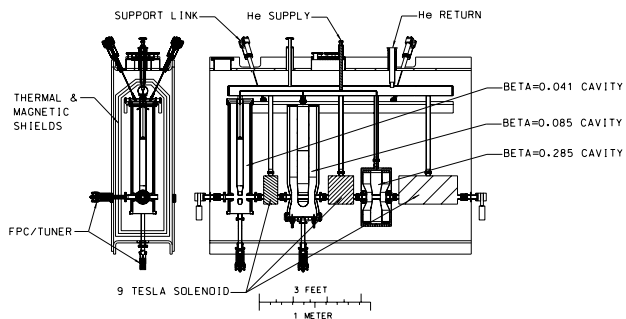


Figure 10: Prototype cryomodule for demonstrating all SCDTL cavities and superconducting solenoids.

OTHER SRF ACTIVITIES

Other areas of interest at MSU include the development of SRF diagnostic devices, research into fundamental causes of nonlinear high field loss (“ Q slope”), and fundamental understanding of niobium material properties. The work in these areas is a collaborative venture between NSCL, the MSU Physics Department, and several engineering departments at MSU. Examples of ongoing work include in situ x-ray imaging of SRF cavities [20] and characterization of high-purity Nb after electron beam welding [21].

CONCLUSION

Superconducting RF activities at MSU are focused on developing elliptical cavities and drift-tube cavities for RIA. By the end of 2004, the cavity R&D will be complete and prototype cryomodules for the various cavity types will be complete. At that time, RIA linac design, costing and production plans, which are critical long-lead items, can be finalized. The RIA post-accelerator will use the same QWRs and cryomodules as the RIA driver linac.

REFERENCES

[1] K. W. Shepard, J. R. Delayen, C. M. Lyneis, J. Nolen, P. Ostroumov, J. W. Staples, J. Brawley, C. Hovater, M. Kedzie, M. P. Kelly, J. Mammosser, C. Pillar, M. Portillo, in *9th Workshop on RF Superconductivity: Proceedings*, p. 345-351.

[2] C. W. Leemann, in *Proceedings of the XX International Linac Conference*, Report SLAC-R-561, 2000, p. 331-335.

[3] K. W. Shepard, in *Proceedings of the 10th Workshop on RF Superconductivity*, p. 313-317.

[4] H. Podlech, U. Ratzinger, D. Gorelov, W. Hartung, F. Marti, X. Wu, R. C. York, in *Proceedings of the Eighth European Particle Accelerator Conference*, 2002, p. 945-947.

[5] D. Gorelov, T. Grimm, W. Hartung, F. Marti, X. Wu, R. C. York, H. Podlech, in *Proceedings of the Eighth European Particle Accelerator Conference*, 2002, p. 900-902.

[6] Proceedings of the RIA Driver Workshop II, Argonne, IL (May 2002).

[7] X. Wu, D. Gorelov, T. Grimm, W. Hartung, F. Marti, R. C. York, in *Proceedings of the XXI International Linac Conference*, 2002, p. 134-136.

[8] A. Facco & V. Zviagintsev, in *9th Workshop on RF Superconductivity: Proceedings*, p. 203-206.

[9] R. Pardo & G. Zinkann, in *9th Workshop on RF Superconductivity: Proceedings*, p. 10-14.

[10] G. Ciovati, P. Kneisel, K. Davis, K. Macha, J. Mammosser, in *Proceedings of the Eighth European Particle Accelerator Conference*, 2002, p. 2247-2249.

[11] W. Hartung, J. Bierwagen, S. Bricker, J. Colthorp, C. Compton, T. Grimm, S. Hitchcock, F. Marti, L. Saxton, R. C. York, A. Facco, V. Zviagintsev, “Niobium Quarter-Wave Resonator Development for the Rare Isotope Accelerator,” these proceedings.

[12] T. L. Grimm, J. Bierwagen, S. Bricker, C. C. Compton, W. Hartung, F. Marti, R. C. York, “Experimental Study of a 322 MHz $v/c = 0.28$ Niobium Spoke Cavity,” presented at the 2003 Particle Accelerator Conference.

[13] D. Barni, G. Ciovati, P. Kneisel, C. Pagani, P. Pierini, P. Ylae-Oijala, Tech Note Jlab-TN-01-014, Jefferson Lab, Newport News, Virginia (2001).

[14] C. C. Compton, T. L. Grimm, W. Hartung, H. Podlech, R. C. York, G. Ciovati, P. Kneisel, D. Barni, C. Pagani, P. Pierini, in *Proceedings of the 2001 Particle Accelerator Conference*, p. 1044-1046.

[15] W. Hartung, C. C. Compton, T. L. Grimm, R. C. York, G. Ciovati, P. Kneisel, “Status Report on Multi-cell Superconducting Cavity Development for Medium-velocity Beams,” presented at the 2003 Particle Accelerator Conference.

[16] T. L. Grimm, W. Hartung, M. Johnson, R. C. York, P. Kneisel, L. Turlington, “Cryomodule Design for the Rare Isotope Accelerator,” presented at the 2003 Particle Accelerator Conference.

[17] T. L. Grimm, W. Hartung, F. Marti, H. Podlech, R. C. York, J. Popielarski, C. Wiess, L. Kempel, G. Ciovati, P. Kneisel, in *Proceedings of the Eighth European Particle Accelerator Conference*, 2002, p. 2241-2243.

[18] Q.-Sh. Shu, J. Susta, G. Cheng, T. Grimm, J. Popielarski, S. Einarson, T. Treado, “Input RF Coupler Windows for RIA Cavities,” these proceedings.

[19] M. Stirbet, J. Popielarski, T. L. Grimm, M. Johnson, “RF Conditioning and Testing of Fundamental Power Couplers for the RIA Project,” these proceedings.

[20] S. E. Musser, T. L. Grimm, W. Hartung, “X-Ray Tomography of Superconducting RF Cavities,” presented at the 2003 Particle Accelerator Conference.

[21] H. Jiang, T. R. Bieler, C. C. Compton, T. L. Grimm, “Mechanical Properties, Microstructure, and Texture of Electron Beam Butt Welds in High Purity Niobium,” presented at the 2003 Particle Accelerator Conference.